

Metastable Pitting on 304 Stainless Steel in Cement Extract Solution with Different Concentration of Cl⁻

Xingguo Feng^{1,2}, Yiwen Xu¹, Xiangying Zhang¹, Xiangyu Lu^{1*}, Ruilong Shi¹, Leyuan Zhang¹, Jing Zhang¹, Da Chen¹

¹ Jiangsu Key Laboratory of Coast Ocean Resources Development and Environment Security, Hohai University, Nanjing 210098, Jiangsu, China

² State Key Laboratory of Green Building Materials, 100024, Beijing, China

*E-mail: luxiangyu@hhu.edu.cn

Received: 7 December 2018 / Accepted: 18 January 2019 / Published: 10 March 2019

Metastable pitting behavior of 304 stainless steels in cement extract solution (pH 8) with various concentration of Cl⁻ was studied by Mott-Schottky plot, potentiodynamic polarization, and potentiostatic polarization, respectively. Nucleation rate and the probability of transformation from metastable to stable pitting on the stainless steel significantly increased when the concentration of Cl⁻ increased. The growth rate and re-passivation rate of individual metastable pitting also increased with the concentration of Cl⁻ in the carbonated cement extract solution. Interestingly, differing from the widely accepted view that the type of metastable pitting is characteristic of the kinds of metals or alloys and the type is not affected by the solution environment, in the present study, the types of metastable pitting on the 304 stainless steel gradually transformed from Type II to Type I when the concentration of Cl⁻ increase in the pore solution. Additionally, high donor density suggests that the passive film has a high susceptible of pitting, but it may enhance the rate of passivation in the subsequent passivation process for the steel in the cement extract.

Keywords: stainless steel; pore solution; metastable pitting; growth rate; re-passivation rate

1. INTRODUCTION

Stainless steels rebar, an effective candidate of high-durability marine structures, could suffered from pitting corrosion in the aggressive environments [1-4]. For Cl⁻ degrades the passive film and induce the initial of pitting corrosion, many attentions have been attracted on the effect of Cl⁻ on pitting corrosion of different types of stainless steels. Hong and co-authors [5] have studied the pitting on 304 stainless steels in neutral Cl⁻ solutions. The results show that the metastable pitting potentials are linear decreased with the logarithm of Cl⁻ concentration in solution. Similarly, Fajardo and co-

authors [6] compared the pitting corrosion resistance of AISI 304 and a low-nickel stainless steel in a carbonated alkaline solution (pH 8) with different concentration of Cl^- . The authors also reported that the pitting potential almost linearly decreased whereas the corrosion potential slightly increased with the logarithm of Cl^- concentration. Pujar and co-authors [7] have investigated the effect of Cl^- ions and sulfate ions on corrosion behavior of 316 stainless steels in deaerated solutions, and the authors suggested that the Cl^- degraded the passive film and induced the stable pitting on the stainless steels, while the sulfate ions strengthen the passivity of the stainless steel in the solution. Zuo and co-authors [8] analyzed the metastable pitting of 316L stainless steels in sodium Cl^- solution and noticed that the growth rate and peak current of metastable pits increased with the concentration of Cl^- , indicating that the metastable pits were accelerated by the increasing concentration of Cl^- . Furthermore, Zuo [8] suggested that the statistical characteristics of metastable pitting also were the effective indicators to estimate the pitting corrosion resistance of metals. However, Pardo [9] noticed that the pitting potential and crevice potential of the high-alloy stainless steel do not show a significant decrease tendency with the increasing concentration of Cl^- in acid solutions with different pH. Pistorius and Burstein [10] also studied the metastable pits on 304 stainless steels in acid (pH 0.7) and neutral (pH 7) solution with different concentration of Cl^- , respectively. The metastable pitting onsets were found to be decreased with the reducing concentration of Cl^- and the increasing dissolved oxygen in solution. In general, the metastable pitting of stainless steel was significantly influenced by Cl^- in solution.

Effect of pH on pitting of stainless steels also has been extensively investigated. Gong and co-authors [11] reported that the metastable pitting potential and stable pitting potential increase, while the nucleation of metastable pits decreases with the value of pH. Simultaneously, the growth rate, peak current and average lifetime of the metastable pits does not be significantly influenced by the pH of solution. Li and co-authors [12] studied the pitting corrosion resistance of an austenitic stainless steel weldment in a simulated concrete pore solution and noticed that the resistance of the weldment was enhanced as the pH of pore solution was increased from 10.5 to 13.5. In addition, Ye and co-authors [13] checked the evolution of single pits on 304 stainless steels in solution with different pH. The authors declared that the pitting current, the growth rate, the pit volume, the pit depth and the diameter of pit mouth of the individual pits increase, whereas the integrity of the lacy cover declines with the decreasing pH.

Many studies also investigated the growth and re-passivation of the individual metastable pitting on various types of stainless steels [14]. Feng and co-authors [15] investigated the metastable pitting on deformed 304 stainless steel in a contaminated concrete pore solution. The results suggested that the carrier density of passive film and the lifetime of metastable pitting increase with the magnitude of deformation, and secondary metastable pitting can be observed on the severely deformed samples. After studying the current transients of metastable pitting on 304 stainless steels in an acid solution containing 0.025 mol L^{-1} hydrogen Cl^- and 0.075 mol L^{-1} perchloric acid, Burstein [16] suggested that the current peaks, corresponding to metastable pitting, presented a slow rise and followed by a sharp fall, which means that the current transients of an individual metastable pitting shows a low growth rate and followed by a high re-passive rate. Similar situation for the metastable pitting on stainless steel in acid or neutral solutions was also reported in other earlier studies [10, 17, 18]. After reviewing the current peaks of metastable pitting on various metals, Soltis [14] divided these

peaks into two types: a low growth rate followed by a high re-passivation rate is defined as Type I, while a high growth rate followed by a low re-passivation rate is defined as Type II. Additionally, the metastable pits on various stainless steels always are Type I, and the pits on pure iron, carbon steel, and low chrome steels mostly are Type II [14, 19]. In the present study, the metastable pitting of 304 stainless steels was investigated in cement extract solution, a simulated concrete pore solution, with different concentration of Cl^- . The results suggest that the types of the metastable pitting were significantly affected by the concentration of Cl^- .

2. MATERIALS AND EXPERIMENTS

2.1 Materials

Plain round (Φ 10 mm) AISI 304 austenitic stainless steel bars, with chemical composition (wt.%): carbon 0.075%, silicon 0.32%, manganese 1.3%, phosphorus 0.02%, sulphur 0.0068%, chromium 18.1%, nickel 8.2%, molybdenum 0.16% and iron for the balance, was used in the present study. Samples having a length of 10 mm were ground by using emery papers with grade 240#, 600# and 1000#, respectively. Copper wires were welded at one end of the steel samples for electrochemical measurement. After being cleaned by deionized water, alcohol, the samples were coated with silica gel, leaving an exposed area of 0.1 cm^2 in the middle of the cross section. The cement extract solution was prepared by mixing the ordinary Portland cement (P.O 42.5) with distilled water in a mass ratio of 1:5. The mixed cement slurry was stirred for 30 min and was held for 4 h, then was filtered [20, 21]. The filtered liquid, with a pH of 12.5, was used to simulate the concrete pore solution. The resistivity of the cement extract solution, tested with a DDST-308A conductivity instrument, was $77.9 \Omega \text{ cm}$. The concentrations of cations and anions in the solution were $5.62 \times 10^{-5} \text{ mol L}^{-1}$ potassium ion, $2.57 \times 10^{-5} \text{ mol L}^{-1}$ calcium ion, $9.83 \times 10^{-5} \text{ mol L}^{-1}$ sodion, $2.16 \times 10^{-5} \text{ mol L}^{-1}$ sulphate, and $7.38 \times 10^{-6} \text{ mol L}^{-1} \text{ Cl}^-$, respectively. To simulate the carbonated concrete pore solution, the pH of the cement extract solution was adjusted to the values of 8 by using a dilute nitric acid solution. The effects of Cl^- on metastable pitting of AISI 304 stainless steels were studied in the cement extract solution separately contained 0.05 mol L^{-1} , 0.5 mol L^{-1} and 5 mol L^{-1} sodium Cl^- .

2.2 Experimental procedure

Electrochemical measurements were conducted by using a CS350 workstation (Corrtest Instrument, China). Ag/AgCl electrode and a platinum plate were separately used as the reference and counter electrode. Every experiment was performed in triplicate at room temperature. These prepared stainless steel samples were polarized at -1.0 V for 5 min before electrochemical experiments [22]. After being exposed 2 h in the cement extract solution, Mott-Schottky plots of the samples were performed between -1.5 and 1.5 V . Basing on our earlier study [23], a frequency of 1000 Hz was suitable for the Mott-Schottky test. Thus, in the present study, the frequency and potential step of the Mott-Schottky plots were chosen at 1000 Hz and 50 mV, respectively. For investigating the metastable pitting potentials (E_m) and the stable pitting potentials (E_b), the potentiodynamic polarizations were

tested at a scan rate of 0.2 mV s⁻¹ in the range from -0.3 ~1.5 V, relative to the open circuit potentials. If stable pitting occurred before the potentials reach to the design values, the potentiodynamic polarization tests were stopped. Potentiostatic polarizations were performed at 0.2 V to record the current transients, and a frequency of 20 Hz is adopted to collect the data.

3. RESULTS AND DISCUSSION

3.1 Semi-conducting properties

Mott-Schottky plots of the 304 stainless steel in the cement extract solutions with different concentrations of Cl⁻ are shown in Figure 1. As the results show, negative slopes were observed when the potential in the range between -1.3 to -0.7 V (*R*₁), suggesting that this film is a p-type semiconducting material [24, 25], and corresponds to the inner Cr₂O₃ film on the stainless steel [26, 27]. When the potentials in ranging from -0.6 to 0 V (*R*₂), positive slopes is observed, indicating a n-type semiconducting film, and it was attributed to the capacitance response of the outer iron oxides layer of the stainless steel [26, 27]. As the potential further increasing, negative slopes are observed again. Dong [28] and Carmezim [29] attributed this situation to the breakdown of the passive film.

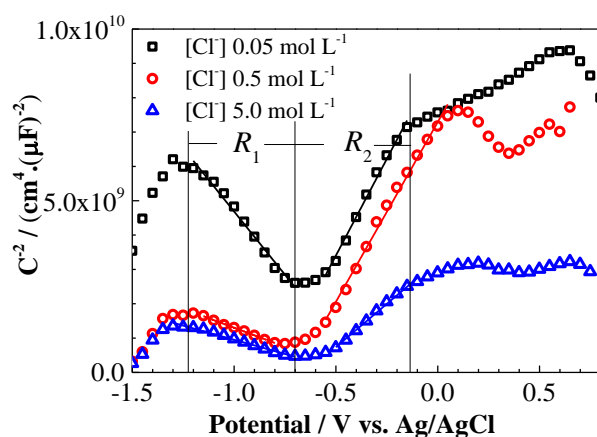


Figure 1. Mott–Schottky plots of 304 stainless steel samples immersed 2 h in the cement extract solutions (pH 8) with different concentration of Cl⁻, at a frequency of 1000 Hz and a potential step of 50 mV.

The hypothesis that the capacitance of the Helmholtz layer (*C_H*) is negligible is acceptable [28]. Based on Mott-Schottky theory [30], the capacitances of n-type and p-type semiconductors are given by Eqs. (1) and (2), respectively:

$$C^{-2} = \frac{2}{\epsilon\epsilon_0qN_D} \left(E - E_{FB} - \frac{kT}{q} \right) \quad (1)$$

$$C^{-2} = \frac{-2}{\epsilon\epsilon_0qN_A} \left(E - E_{FB} - \frac{kT}{q} \right) \quad (2)$$

where *N_A* and *N_D* is the acceptor density and donor density; ϵ and ϵ_0 is the permittivity of free space and the dielectric constant of the passive film, respectively (ϵ is 15.6 [23, 24]); *E* is the applied potential; *E_{FB}* is flat band potential, can be got from the extrapolation for *C*⁻² = 0; *q* is the electron

charge; k is the Boltzman constant; T is the absolute temperature, and kT/q was neglected as it is only ~ 25 mV at room temperature) [31].

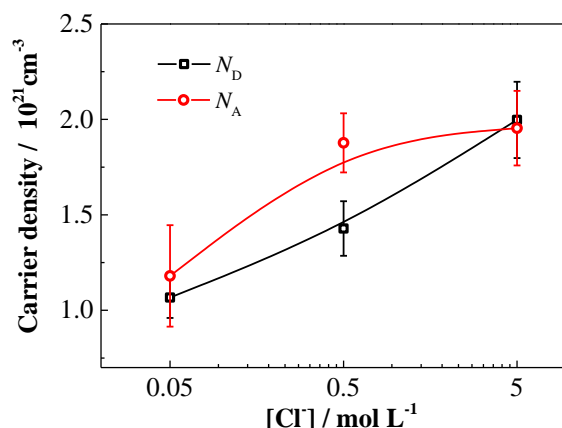


Figure 2. Variation of donor (N_D) and acceptor (N_A) densities of 304 stainless steels in the cement extract solutions (pH 8) with different concentration of Cl^- ion.

The results of the N_A , N_D are presented in Figure 2. As the results show, the carrier density of the passive film on the stainless steel is approximately in the order of magnitude $1\sim 2 \times 10^{21} \text{ cm}^{-3}$, consistent with the earlier report from Ferreira [32], which suggested the carrier density of passive film is about $5 \times 10^{20} \text{ cm}^{-3}$ at room temperature (25 Celsius degree). Moreover, it is easy to notice that the carrier density significantly increased with the increasing concentration of Cl^- . As many studies have confirmed, a high donor density means a low stability of passive films and a high sensitive of pitting [33-36]. Consequently, the results in Figure 2 suggest that the un-stability of the passive film and the pitting sensitive of the stainless steel increased with the increasing concentration of Cl^- .

Furthermore, the thickness of the space-charge layer (d) is determined by the applied potential (E) and flat band potential according to Eqs. (3) [37], and the results are shown in Figure 3.

$$d = \left[\frac{2\epsilon\epsilon_0}{qN} \left(E - E_{FB} - \frac{kT}{q} \right) \right]^{\frac{1}{2}} \quad (3)$$

As the results (Figure 3) show, the thickness of the space-charge layer significantly declined with the increasing concentration of Cl^- . Similarly, Valéria [36] had studied the passive films on different mild steels in sodium bicarbonate solution, and the authors noticed that the space charge layers of the samples in the solution contained $0.01 \text{ mol L}^{-1} \text{ Cl}^-$ were obvious thinner than the counterparts in solution without Cl^- . Simultaneously, as Figure 3 shows, the space charge layers became thinner and the passive films were more heavily doped (Figure 2) when the concentration of Cl^- increased. This situation suggests that the sensitive of pitting on the stainless steel increased with the increasing concentration of Cl^- of the alkaline cement extract solution [37].

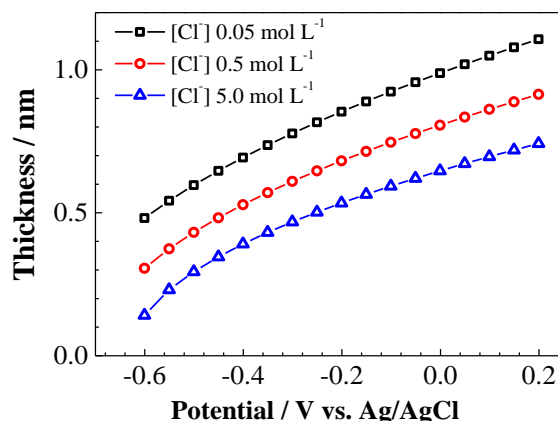


Figure 3. The thickness of the space charge layers of 304 stainless steel in the cement extracts solutions (pH 8) with different Cl^- concentration.

3.2 E_m and E_b

Potentiodynamic polarization curves of AISI 304 stainless steels in pore solution with different concentration of Cl^- are shown in Figure 4. Many current fluctuations, corresponding to the metastable pitting, in the anodic regions can be observed. According to Tang [38], the peak of current fluctuation higher than $0.02 \mu\text{A cm}^{-2}$ is the sign of an individual metastable pitting. Moreover, the potential corresponding to the first metastable pitting was defined as the metastable pitting potential E_m . The potential, corresponding to the peak of current continually and sharply increases without decaying back to the background level, was defined as pitting potential E_b . As the results show, more metastable pitting can be observed in the anodic region when the concentration of Cl^- increased.

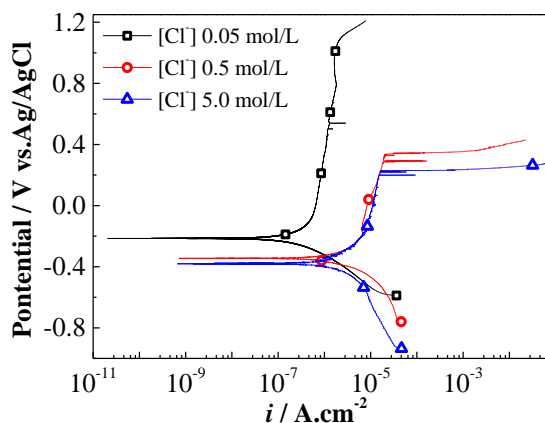


Figure 4. Potentiodynamic polarization curves of the 304 stainless steel samples in pore solutions with various concentration of Cl^- , as measured at a scan rate of 0.2 mV s^{-1}

Results of E_m and E_b in pore solution with different concentrations of Cl^- are presented in Figure 5. As the results show, both E_m and E_b linearly decreased with the logarithm of Cl^-

concentration, which is consistent with the results in previous studies [5, 38]. According to Organ [39] and Ernst [40], the nucleation and growth of the metastable pitting may be accelerated by Cl^- . Moreover, the transition from metastable to stable pitting was also promoted by Cl^- in solution. On the other hand, Punck and co-authors [41] attributed the stable pitting to the strong interaction among metastable pitting. When the density of metastable pitting exceeds a critical value, the strong interaction will promote many metastable pitting suddenly occurred on a local area, and then the stable pitting formed on the area. In the present study, more current peaks of metastable pitting can be observed in the anodic regions (Figure 5) for the ones immersed into cement extract solution with higher concentration of Cl^- . This result, together with the carry density results (Figure 3), confirmed that the nucleation of metastable pitting was accelerated by the increasing concentration of Cl^- .

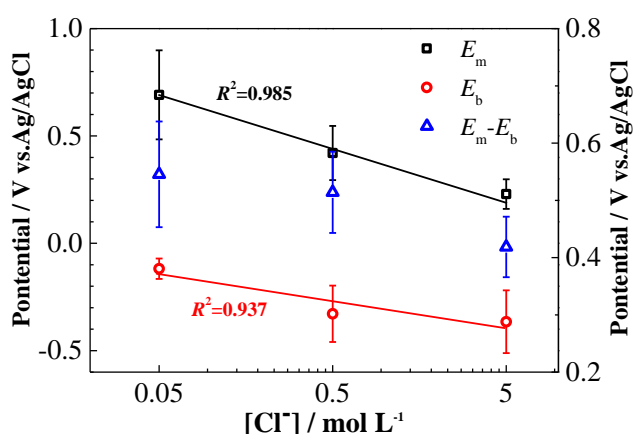


Figure 5. E_m , E_b and $(E_b - E_m)$ of 304 stainless steel in cement extract solutions (pH 8) with concentration of Cl^- .

The gaps between E_m and E_b were further investigated and the results are presented in Figure 5. As the results show, the value of $(E_b - E_m)$ obviously decreased with the increasing concentration of Cl^- of the pore solution. According to earlier studies [38, 42], the differences between E_m and E_b was related to the transformation probability from the metastable to stable pitting as well as the repassivation ability of metals in solution. After investigating the E_m and E_b of Q235 steel, X70 steel, pure iron and 316L stainless steel in Cl^- solutions, Tang and co-authors noticed that the gap between E_m and E_b of 316L stainless steel is much higher than that of the other steel[36]. Moreover, the E_b of these studied metals linearly increased with the E_m , and the slopes of the straight line increased with the concentration of Cl^- in solution. Thus, the authors suggested that the gaps between E_m and E_b play the key role in both the nucleation processes of metastable pitting and stable pitting. The results in Figure 5, together with the Mott-Schottky results (Figure 2, Figure 3), indicating that the probability of metastable translated to the stable pitting increased with the increasing concentration of Cl^- and the declining of pH in pore solution.

3.3 Potentiostatic polarization

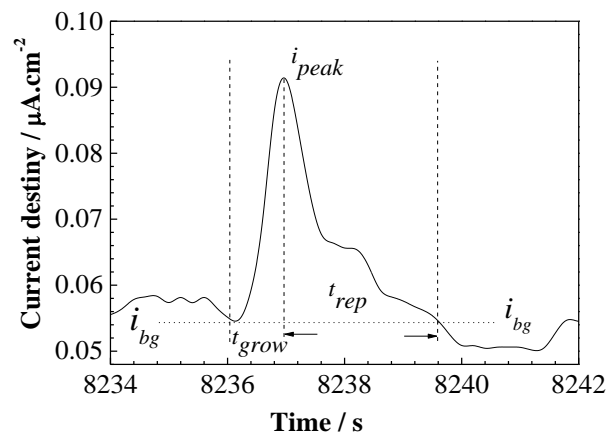


Figure 6. Typical current transients of metastable pits formed on 304 stainless steel in the carbonated cement extract solutions (pH 8) with $0.5 \text{ mol L}^{-1} \text{ Cl}^-$, potentiostatic polarization at 0.2 V.

As the potentiodynamic polarization curves (Figure 4) show, many current fluctuations can be observed when the applied anodic potentials higher than -0.1 V , which are related to metastable pitting events on the surface [36]. As the potentials exceed 0.3 V , the current density continuously increased, which indicated that stable pitting occurred on the surface of steel. Thus, potentiostatic polarizations were performed at 0.2 V [43, 44] to record the current transients in the present study. Typical current transients of 304 stainless steel in the carbonated pore solution with a pH of 8 and $0.5 \text{ mol L}^{-1} \text{ Cl}^-$ are presented in Figure 6. The parameters shown in Figure 6 are defined as follow: t_{grow} and t_{rep} are the growth time and re-passivation time of a metastable pit; i_{peak} is the peak current densities; i_{bg} is the background current and hence; $(i_{\text{peak}} - i_{\text{bg}})$ corresponds to the peak current density of metastable pitting [15]. According to previous studies, the growth and re-passivation rate (K_{grow} and K_{rep} , respectively) of the metastable pits are determined from the peak current density ($i_{\text{peak}} - i_{\text{bg}}$) and time, as follow [14, 18, 45, 46]:

$$K_{\text{grow}} = \frac{(i_{\text{peak}} - i_{\text{bg}})}{t_{\text{grow}}} \quad (5)$$

$$K_{\text{rep}} = \frac{(i_{\text{peak}} - i_{\text{bg}})}{t_{\text{rep}}} \quad (6)$$

Typical current transient of 304 stainless steel in the carbonated cement extract solution (pH=8) with different concentrations of Cl^- are shown in Figure 7. As the results show, the background current i_{bg} and the peak current i_{peak} significantly increased with the concentration of Cl^- in solution. Moreover, the i_{bg} obviously decreases with the polarization time for the samples in the solutions with low concentration of Cl^- (Figure 7 (a), (b)), indicating the stainless steel gradual passivation in the solutions [47]; while it does not show significant change for the ones in the solution with the highest concentration of Cl^- (5 mol L^{-1} , Figure 7 (c)), suggesting the samples can't passivation in the solution.

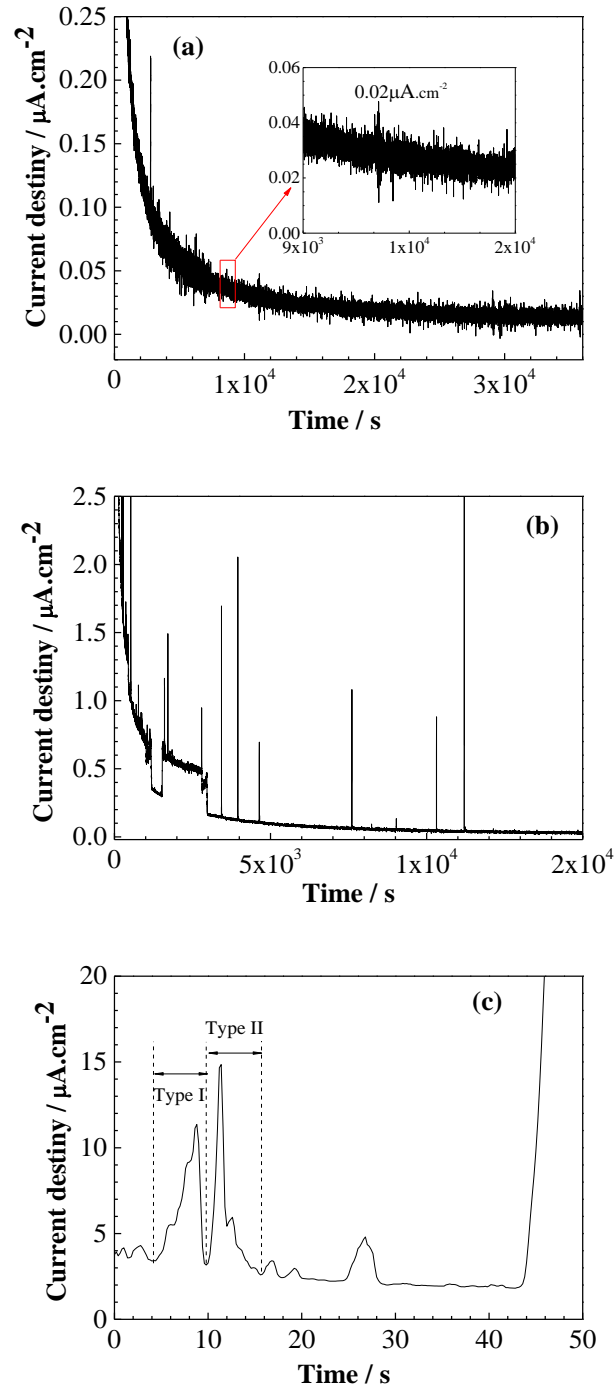


Figure 7. Typical current transients of metastable pits formed in 304 stainless steel in the carbonated cement extract solutions (pH 8) with different concentration of Cl^- , potentiostatic polarization at 0.2 V; (a) 0.05 mol L^{-1} , (b) 0.5 mol L^{-1} , (c) 5 mol L^{-1} .

On the other hand, it is easy to notice that the incubation time of the stable pitting dramatically reduce with the concentration of Cl^- increasing. This situation directly confirms that the transformation probability from metastable to stable pitting of the stainless steel was significantly increased with the concentration of Cl^- in cement extract solution [40].

3.4 Statistical characteristics of metastable pitting

The dependence of the growth and re-passivation rates of individual metastable pitting on the current density peak is shown in Figure 8. As the results show, the growth and re-passivation rates obviously increased with the value of the current density peak. Meanwhile, the K_{grow} and K_{rep} dramatically increase with the concentration of Cl^- in the cement extract solution. In the case of the sample exposed to the solution with $0.05 \text{ mol L}^{-1} \text{ Cl}^-$, almost all the K_{grow} and K_{rep} of individual metastable pitting are below $0.2 \mu\text{A} (\text{cm}^2 \cdot \text{s})^{-1}$. However, for the sample in the solution of $0.5 \text{ mol L}^{-1} \text{ Cl}^-$, most of the K_{grow} and K_{rep} locate between 0.5 to $3 \mu\text{A} (\text{cm}^2 \cdot \text{s})^{-1}$. The magnitude of K_{grow} and K_{rep} reach to $\sim 10 \mu\text{A} (\text{cm}^2 \cdot \text{s})^{-1}$ when the concentration of Cl^- further increased to 5.0 mol L^{-1} . Similarly, Zuo [8] and Blanc [48] have investigated the metastable pitting on stainless steel and aluminum alloy in solution with different concentration of Cl^- , respectively. They also noticed that the growth rate of metastable pitting increased with the increasing concentration of Cl^- . It is well accepted that the diffusion of dissolving metal cations in the pit constitutes the rate-controlling step for the growth of the metastable pit [15, 49], and the metal cations would counterbalance the ingress of anions in the pit. For the samples immersed in the solution with high concentration of Cl^- , the diffusion rate of the anions (Cl^-) is higher, which may accelerate the diffusion of the cations. Thus, the growth rates of the metastable pitting are increased with the concentration of Cl^- .

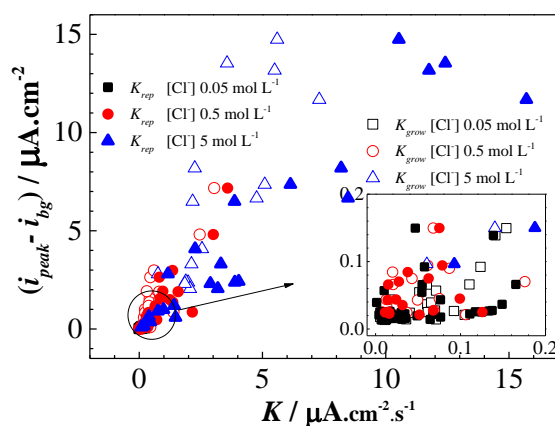
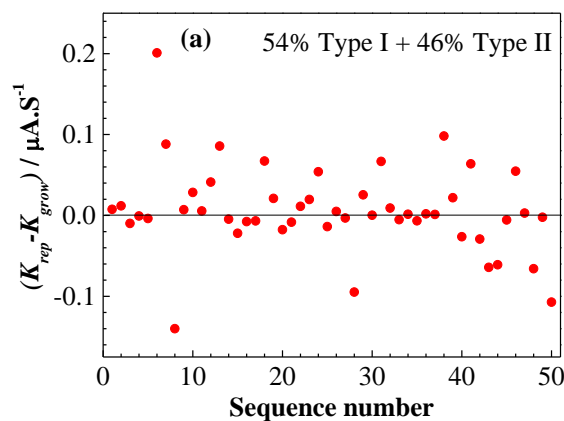


Figure 8. Influence of the concentration of Cl^- on the K_{grow} and K_{rep} in the carbonated cement extract solutions (pH 8).

On the other hand, as the metastable pitting grow to a certain depth, the further growth was limited by the transport of Cl^- from the bulk electrolyte down the electrolyte channel to the substrate at the bottom of the pits. Thereafter, the diffusion of dissolving metal cations in the pits was hindered and the metastable pitting started to re-passivation [10]. Many authors reported [17, 50], that the rupture of the flawed cover over the pit mouth is essential to the re-passivation of metastable pits. In general, there would be higher concentration of Cl^- fill into the pits as the flawed cover layer cracking for the samples in the high concentration of Cl^- bulk solution. Thus, as the results show in Figure 1 (a), the higher concentration of Cl^- in the pit may promote the film formed during initial re-passivation contained higher density of donor. According to the point defect model (PDM) [34, 35], the donor

density is related to the oxygen vacancy concentration in the film. The higher concentration of oxygen vacancy could promote the migration of oxygen in the film and accelerate the passivation of substrate at the metal/film interface in the pits. Consequently, as the results in Figure 9 shows, the re-passivation rates of the metastable pitting also increased with the concentration of Cl^- in the pore solution in the present study. It is worthy to notice that the high re-passivation rate does not mean the high stability of the formed passive film. Coincidentally, our earlier studies have investigated the passive behavior of deformed carbon steel in pore solution without Cl^- [47] and the re-passivation characters of metastable pitting on deformed stainless steel in pore solution with low concentration of Cl^- [15], respectively. The results suggested that the donor densities in the passive films of the two steels increased with the magnitude of deformation, and the passivation rate (or re-passivation rate) also increased with the concentrations of donor densities in the films [15, 47]. The activity of the substrate can be enhanced by the increasing dislocations under highly deformation, which leads to the enrichment of iron ions and faster formation of the passive film [15, 47, 51]. Simultaneously, some authors suggested that the migration of oxygen vacancy dominates the transport process in the passive film, which is the critical step for the growth of passive film [14, 34, 35]. Especially, in the present study, the high concentration of Cl^- in bulk pore solution led the passive film to be heavily doped (Figure 2), whereas does not change the microstructure of substrate. However, as the results shown in Figure 2 and Figure 8, the re-passivation rate of the metastable pitting also increased with the concentration of oxygen vacancy. This situation, together with the effect of donor density on passivation of steels in pore solution in earlier studies [15, 47], suggesting that the high donor density can enhance the passivation rate of steel in pore solution.



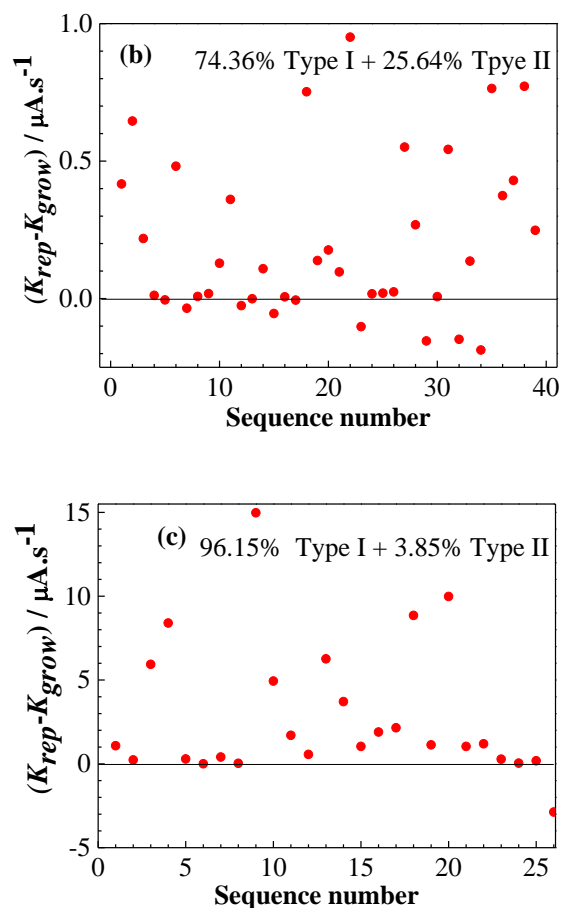


Figure 9. Difference of values of K_{rep} and K_{grow} in the carbonated cement extract solution (pH 8) with different Cl^- concentration; (a) 0.05 mol L^{-1} , (b) 0.5 mol L^{-1} , (c) 5 mol L^{-1} .

Finally, effect of the concentration of Cl^- on the type of metastable pitting was investigated, and the results are presented in Figure 9. Generally, two types of metastable pitting were reported in the literature [14, 16, 52]: the Type I is distinguished by a low growth rate, followed by a high re-passivation rate of the pit, whilst the Type II displays a high growth rate followed by a low re-passivation rate (as shown in Figure 7 (c)). In addition, the types of metastable pitting are characteristic of the kinds of metals or alloys. The Type I is the typical characteristics of metastable pitting on various stainless steels, while the Type II is that for pure iron, carbon steel, and the low chromium steels [14, 19]. Then, according to the literature [14], it is easy to know that the metastable pitting on stainless steel generally presented a low grow rate followed by a high re-passivation rate, which means that the re-passivation rate could always higher than the growth rate in the same individual metastable pits. However, as the results in Figure 9 shows, the types of the metastable pitting are significantly influenced by the concentration of Cl^- in the simulated pore solution. In the case of the sample exposed to the cement extract solution with the lowest concentration of Cl^- (0.05 mol L^{-1}), about half (~46%) of the current transients of the metastable pitting on the stainless steel is presented Type II, (Figure 9(a)). This result is obvious different from the results reported in the literature, which suggested that the metastable pitting on stainless steel dominated by Type I [14, 16, 19]. The difference may have

resulted from the chemical composition of the cement extract solutions as it contained some potassium, calcium, sodium ions and silicate [15], which is different from the aqueous solution with Cl^- [16]. Similarly, Veleva and co-authors [53] have reported that better passivation of an AISI316 stainless steel in the cement extract than in a saturated calcium hydroxide solution. As the concentration of Cl^- increases (0.5 mol L^{-1}), the ratio of the Type II metastable pitting gradually reduces, and about 25% metastable pitting can be divided into Type II (Figure 9(b)). As the concentration of Cl^- further increases (5.0 mol L^{-1}), the Type II metastable pitting almost disappeared for the stainless steel exposed to the cement extract solution (Figure 9(c)). Consequently, it is easy to conclude that there are two types of metastable pitting for the stainless steel exposed to the cement extract solution with low concentration of Cl^- . As the concentration of Cl^- in the pore solution increasing, the Type II metastable pitting decreased, whereas the Types I increased on the 304 stainless steel, and the metastable pitting gradually transforms from Type II to Type I.

4. CONCLUSIONS

The metastable pitting on AISI 304 stainless steels in the cement extract solution was studied by using Mott-Schottky plot, potentiodynamic polarization, and potentiostatic polarization, respectively. The following conclusions can be drawn from the results of this study.

(1) The carrier densities of the passive film on the stainless steel increased, while the thickness of the space charge layers decreased with the increasing concentration of Cl^- in the cement extract solution.

(2) The metastable pitting potentials (E_m), the stable pitting potentials (E_b), as well as the gap between E_b and E_m significantly decreased with the increasing concentration of Cl^- in the cement extract solution, which suggests that the nucleation rate and transformation probability from metastable to stable pitting of the stainless steel was significantly increased with increasing concentration of Cl^- .

(3) In the carbonated cement extract solution ($\text{pH}=8$), as the concentration of Cl^- increasing, the growth rate and the re-passivation rate of the individual metastable pitting significantly increased. Simultaneously, the type of metastable pitting also changed from a high growth rate followed by a low re-passivation rate (Type II) to a low growth rate followed by a high re-passivation rate (Type I). For stainless steel exposed to the concrete pore solutions, the high donor density in the initial film could accelerate the subsequent passivation rate of the steels.

ACKNOWLEDGEMENTS

The authors are grateful to the National Natural Science Foundation of China (51601074), the Fundamental Research Funds for the Central Universities (2018B56714), the Opening Project of State Key Laboratory of Green Building Materials, and the Key Laboratory of Marine Materials and Related Technologies, Ningbo Institute of Materials Technology and Engineering, Chinese Academy of Sciences (Grant. 2017K08).

References

1. G.T. Burstein, C. Liu, R.M. Souto and S.P. Vines, *Br. Corros. J.*, 39 (2004) 25.
2. C.H. Jiang, K. Fan, F. Wu and D. Chen, *Mater. Design*, 58 (2014) 187.
3. G.T. Burstein, R.M. Souto, C. Liu and S.P. Vines, *Corros. Mater.*, 29 (2004) 1.
4. Y. Hou, C.Q. Cheng, T.S. Cao, X.H. Min and J. Zhao, *Int. J. Electrochem. Sci.*, 13 (2018) 7095.
5. T. Hong and M. Nagumo, *Corros. Sci.*, 39 (1997) 285.
6. S. Fajardo, D.M. Bastidas, M. Criado and J.M. Bastidas, *Electrochim. Acta*, 129 (2014) 160.
7. M.G. Pujar, T. Anita, H. Shaikh, R.K. Dayal and H.S. Khatak, *J. Mater. Eng. Perform.*, 16 (2007) 494.
8. Y. Zuo, H.O. Du and J. Xiong, *J. Mater. Sci. Technol.*, 16 (2000) 286.
9. A. Pardo, E. Otero, M.C. Merino, M.D. López, M.V. Utrilla and F. Moreno, *Corros.*, 56 (2000) 411.
10. P.C. Pistorius and G.T. Burstein, *Corros. Sci.*, 36 (1994) 525.
11. X.Z. Gong, J. Xiao, Y. Zuo, J.M. Zhao and J.P. Xiong, *Journal of Beijing University of Chemical Technology*, 29 (2002) 29. (in Chinese)
12. L. Li, C.F. Dong, K. Xiao, J.Z. Yao and X.G. Li, *Constr. Build. Mater.*, 68 (2014) 709.
13. C. Ye, N. Du, W.M. Tian, Q. Zhao and L. Zhu, *Journal of Chinese Society for Corrosion and Protection*, 35 (2015) 38. (in Chinese)
14. J. Soltis, *Corros. Sci.*, 90 (2015) 5.
15. X.G. Feng, X.Y. Lu, Y. Zuo, N. Zhuang and D. Chen, *Corros. Sci.*, 103 (2016) 223.
16. G.T. Burstein, P.C. Pistorius and S.P. Mattin, *Corros. Sci.*, 35 (1993) 57.
17. G.S. Frankel, L. Stockert, F. Hunkeler and H. Boehni, *Corros.*, 43 (1987) 429.
18. D.E. Williams, J. Stewart and P.H. Balkwill, *Corros. Sci.*, 36 (1994) 1213.
19. D.E. Williams, C. Westcott and M. Fleischmann, *J. Electrochem. Soc.*, 132 (1984) 1804.
20. B. Díaz, L. Freire, X.R. Nóvoa and M.C. Pérez, *Electrochim. Acta*, 54 (2009) 5190.
21. P. Ghods, O.B. Isgor, G. Mcraeb and T. Miller, *Cem. Concr. Compos.*, 31 (2009) 2.
22. X.C. Han, L. Jun, K.Y. Zhao, W. Zhang and S. Jie, *J. Iron. Steel. Res. Int.*, 20 (2013) 74.
23. X.G. Feng, X.Y. Lu, Y. Zuo and D. Chen, *Corros. Sci.*, 82 (2014) 347.
24. Y.F. Cheng and J.L. Luo, *Electrochim. Acta*, 44 (1999) 2947.
25. Z.C. Feng, X.Q. Cheng, C.F. Dong, L. Xu and X. Li, *Corros. Sci.*, 52 (2010) 3646.
26. N.B. Hakiki, S. Boudin and B. Rondot, *Corros. Sci.*, 37 (1995) 1809.
27. H. Tsuchiya, S. Fujimoto and O. Chihara, *Electrochim. Acta*, 47 (2002) 4357.
28. Z.H. Dong, W. Shi and X.P. Guo, *Electrochim. Acta*, 56 (2011) 5890.
29. M.J. Carmezim, A.M. Simoes, M.F. Montemor and M.D.C. Belo, *Corros. Sci.*, 47 (2005) 581.
30. F. Gaben, B. Vuillemin and R. Oltra, *J. Electrochem. Soc.*, 151 (2004) 595.
31. L. Hamadou, A. Kadri and N. Benbrahim, *Appl. Surf. Sci.*, 252 (2005) 1510.
32. M.G.S. Ferreira, N.E. Hakiki, G. Goodlet, S. Faty, A.M.P. Simões and M.D.C. Belo, *Electrochim. Acta*, 46 (2001) 3767.
33. N. Li, Y. Li, S. Wang and F. Wang, *Journal of Chinese Society for Corrosion and Protection*, 27 (2007) 80. (in Chinese)
34. C.Y. Chao, L.F. Lin and D.D. Macdonald, *J. Electrochem. Soc.*, 128 (1981) 1187.
35. D.D. Macdonald, *J. Electrochem. Soc.*, 139 (1992) 3434.
36. V.A. Valéria and C.M.A. Brett, *Electrochim. Acta*, 47 (2002) 2081.
37. G. Okamoto, *Corros. Sci.*, 4 (1973) 471.
38. Y.M. Tang, Y. Zuo, J.N. Wang, X.H. Zhao, B. Niu and B. Lin, *Corros. Sci.*, 80 (2014) 111.
39. L. Organ, Y. Tiwary, J.R. Scully, A.S. Mikhailov and J.L. Hudson, *Electrochim. Acta*, 52 (2007) 6784.
40. P. Ernst and R.C. Newman, *Corros. Sci.*, 44 (2002) 943.
41. C. Punck, M. Bölscher, H.H. Rotermund, A.S. Mikhailov, L. Organ and N. Budiansky, *Science*, 350 (2004) 1133.

42. J.N. Wang; Study of electrochemical feature on pitting early stage for several stages, *Beijing University of Chemical Technology*, Beijing, 2013. (in Chinese)
43. J.B. Lee and S.I. Yoon, *Mater. Chemis. Phys.*, 122 (2010) 194.
44. L. Guan, B. Zhang, X.P. Yong, J.Q. Wang, E.H. Han and W. Ke, *Corros. Sci.*, 93 (2015) 80.
45. W.M. Tian, N. Du, S.M. Li, S.B. Chen and Q.Y. Wu, *Corros. Sci.*, 85 (2014) 372.
46. L. Guan, Y. Zhou, B. Zhang, J.Q. Wang, E.-H. Han and W. Ke, *Int. J. Electrochem. Sci.*, 11 (2016) 2326.
47. X.G. Feng, Y. Zuo, Y.M. Tang, X.H. Zhao and J.M. Zhao, *Corros. Sci.*, 65 (2012) 542.
48. C.Blanc and G.Mankowski, *Corros. Sci.*, 40 (1998) 411.
49. P.C. Pistorius and G.T. Burstein, *Philos. Trans. R. Soc. A*, 341 (1992) 531.
50. P.C. Pistorius and G.T. Burstein, *Mater. Sci. Forum.*, 111 (1992) 429.
51. J.H. Gerretsen and J.H.W. Dewit, *Electrochim. Acta*, 36 (1991) 1465.
52. S.T. Pride, J.R. Scully and J.L. Hudson, *J. Electrochem. Soc.*, 141 (1994) 3028.
53. L. Velea, M.A. Alpuche-Aviles, K. Melissa, B. Graves and W.O. David, *J. Electroanal. Chem.*, 578 (2005) 45.

© 2019 The Authors. Published by ESG (www.electrochemsci.org). This article is an open access article distributed under the terms and conditions of the Creative Commons Attribution license (<http://creativecommons.org/licenses/by/4.0/>).